ATOMISATION IN TURBULENT FLOWS: MODELLING FOR APPLICATION

Novid Beheshti, Alexey A. Burluka
School of Mechanical Engineering,
The University of Leeds, Leeds, LS2 9JT, United Kingdom
N.Beheshti@leeds.ac.uk, A.A.Burluka@leeds.ac.uk

Michael Fairweather
Department of Chemical Engineering,
The University of Leeds, Leeds, LS2 9JT, United Kingdom
M.Fairweather@leeds.ac.uk

ABSTRACT

Sensitivity of predictions obtained with the atomisation model suggested recently, Vallet *et al.* (2001), to a choice of a particular turbulence model has been tested. Three different $k-\varepsilon$-type turbulence models, standard, RNG and one including pressure gradient-velocity correlation, have been applied for a test case of air-assisted atomisation. The results show that the pressure gradient-velocity correlation is important and it allows good agreement with experiments for predicted SMD values on the jet axis to be obtained. However, all the models tested underpredict the spray jet spread rate.

INTRODUCTION

Atomisation, that is reduction of the characteristic size of liquid-containing structures, is involved in the working processes of numerous devices ranging from a domestic aerosol to an oil-fired boiler in a power station, Lefebvre (1989). Atomisation results in an increase in the liquid surface area which defines the rate of vaporisation, so in combusting flows atomisation may become the rate defining process. However, in spite of its importance, the description of atomisation remains largely at the level of semi-empirical formulæ adjusted for a particular type of injector. Partly, this is because the rate of atomisation and the size of droplets produced depends on a priori unknown turbulence properties; however these properties are affected by the presence of a liquid phase, which is usually much denser than the gas, or by gas density changes provoked by the heat release from combustion. Thus, modelling faces two challenges: one is to describe the turbulence in a flow with density variations which could be as great as 700 times (water/cold air), and the second is how to find the extent of atomisation under given turbulence conditions.

A recent paper (Vallet *et al.*, 2001) presented a rather simple, two-equation model which addresses the second task. This model employs two transport equations, one for the average liquid mass fraction, and the second for the mean area of the liquid-gas interface per unit mass of media. It has been noted in that paper that a standard $k-\varepsilon$model could be inadequate for two-phase flows, with solution having been sought through the use of ASM-type models. The present work is devoted to further research on an appropriate choice of turbulence model for two-phase flows, reflecting, in particular, its ability to predict correctly the extent of atomisation through the model of Vallet *et al.* (2001).

ATOMISATION MODEL

The main idea of the approach proposed by Vallet *et al.* (2001) is to consider two-phase mixture as a single continuum where the liquid phase is described similarly to one of species in a multi-component homogeneous reacting mixture. If we introduce the mass of liquid phase *per unit mass of two-phase media* which is denoted as $\widetilde{Y_{liq}}$ then its transport equation can be derived as:

$$\frac{\partial\bar{\rho}\widetilde{Y_{liq}}}{\partial t}+\frac{\partial\bar{\rho}\widetilde{u_j}\widetilde{Y_{liq}}}{\partial x_j}=\frac{\partial}{\partial x_j}\bar{\rho}\frac{D_T}{Sc_{liq}}\frac{\partial\widetilde{Y_{liq}}}{\partial x_j}-\dot{m}_{vap}\bar{\rho}\sigma \qquad (1)$$

where $\dot{m}_{vap}$ is the mean vaporisation rate *per unit surface*, and σ is the mean surface area of the gas-liquid interface *per unit mass of two-phase media*. Turbulent diffusion is expressed in Eq. (1) with the turbulent diffusivity D_T though more refined representations can be used, see e.g. Borghi (1988). The last term in Eq. (1) is the source term describing the vaporisation and its particular form comes from a certain analogy with turbulent combustion modelling, where the notion of the flame surface is introduced. Similarly, in this approach, average vaporisation rate is assumed to be proportional to liquid surface area σ which is calculated from its own transport equation. However, it should be noted that in a sub-critical liquid-gas flow the separation between gas and liquid is really a surface so it is quite legitimate to speak about its area, while a turbulent flame has always a *finite* thickness and therefore definition of a flame area becomes ambiguous.

The transport equation for the average area of liquid-gas interface per unit mass of the two phase mixture is postulated as:

$$\frac{\partial\bar{\rho}\tilde{\sigma}}{\partial t}+\frac{\partial\bar{\rho}\widetilde{u_j}\tilde{\sigma}}{\partial x_j}=\frac{\partial}{\partial x_j}\bar{\rho}\frac{D_T}{Sc_\sigma}\frac{\partial\tilde{\sigma}}{\partial x_j}+\frac{\bar{\rho}\tilde{\sigma}}{\tau_c}\left[1-\frac{\tilde{\sigma}}{\sigma_{eq}}\right] \qquad (2)$$

where τ_c is the characteristic time of the surface production, and the equilibrium interface area is related to the equilibrium droplet size by:

$$\begin{aligned}\sigma_{eq} &= \frac{3\widetilde{Y_{liq}}}{\rho_{liq}r_{eq}}\\ r_{eq} &= Cr\cdot\left(\frac{\bar{\rho}\widetilde{Y_{liq}}}{\rho_{liq}}\right)^{2/15}\frac{\eta^{3/5}}{\varepsilon^{3/5}\rho_{liq}^{3/5}}\end{aligned} \qquad (3)$$

The notion of an equilibrium as applied to a gas-liquid turbulent flow probably deserves further explanation. It is assumed that if at time $t=0$ some liquid is placed into a

gas flow with constant turbulence properties then the liquid phase pattern will tend to a monodispersed spray as time increases. The characteristic time for this relaxation of the liquid shape towards the equilibrium monodisperse spray is τ_c. The size of droplets r_{eq} in this asymptotic state of the monodispersed spray will be such that equilibrium is attained between the mechanisms responsible for droplet break-up, such as the shear actions of fluctuating or mean velocity gradients or droplet collisions, and coalescence.

Note on the Weber number

Weber number is the ratio of flow kinetic energy available to break the liquid ligament to the energy necessary to do it. For most turbulent flows of practical relevance, the Weber number is defined in terms of an average velocity and the flow dimension, and is much greater than one; the Weber number $We_t = \frac{\rho_g u'^2 l_t}{\eta}$ defined in terms of the rms turbulent velocity fluctuation u' and the integral scale of turbulence l_t is also much greater than one. The model of Eqs. (1-3) was formulated assuming that the latter Weber number is infinite. It is quite common to see a definition of Weber number with the droplet size taken as the characteristic length; however all these definitions ignore the fact that the energy of shear motion experienced by a small droplet comes only from the high wavenumber part of the turbulence spectrum. Thus, if the droplet size r_d corresponds to the inertial $k^{-5/3}$ interval, then the velocity difference contributing to the shear over the droplet may be estimated as

$$\langle \Delta v(r_d) \rangle \approx (\varepsilon r_d)^{1/3} \approx u' \cdot \left(\frac{r_d}{l_t}\right)^{1/3} << u'$$

If the droplet size is comparable to the Kolmogorov microscale l_K then the corresponding velocity difference will be of order $(\varepsilon\nu)^{1/4}$.

Constructing the Weber numbers in terms of the appropriate velocity differences rather than integral values allowed Kolmogorov (1949) to explain experimentally observed values of r_{eq} in turbulent flows of two liquids of nearly equal densities. However, application of the same principles to gas-liquid flows results in equilibrium droplet radii of several mm while experimental values would be two orders of magnitude smaller. The Weber numbers calculated from the experimental values would then be much less than one, which means that the hydrodynamic shear (neither mean nor fluctuating) is not an effective mechanism of droplet break-up in gas-liquid flows.

Vallet *et al.* (2001) suggested that droplet collision is the mechanism for droplet break-up, as an alternative to hydrodynamic shear. This assumption yields the droplet sizes consistent with experimental observations and results in Eq. (3) for equilibrium droplet size.

Atomisation rate

In addition to presuming equilibrium, one needs as well the rate at which the flow relaxes towards it. The possibilities are to assume τ_c proportional to

- the integral time scale of turbulence,

$$\tau_c = C_1 \cdot \frac{\tilde{k}}{\tilde{\varepsilon}} \tag{4}$$

- characteristic mean velocity time,

$$\tau_c = C_2 \cdot \left(\left(\frac{\partial \tilde{u}_i}{\partial x_j} + \frac{\partial \tilde{u}_j}{\partial x_i} \right)^2 \right)^{-\frac{1}{2}} \tag{5}$$

  Use of these two expressions implies that the rate of the interface surface area generation is determined by large scale turbulent motion. In cases where the liquid is contained in the form of droplets and the surface production or destruction is caused by droplet break-up or coalescence during collisions, these equations imply that collisions between droplets occur on the boundaries of large-scale vortices.

- characteristic droplet collision time,

$$\tau_c = C_3 \cdot \frac{(36\pi)^{2/9}}{\tilde{\varepsilon}^{1/3}} \cdot \left(\frac{\bar{\rho}\tilde{Y}_{liq}}{\rho_{liq}} \right)^{4/9} \cdot \frac{1}{(\bar{\rho}\tilde{\sigma})^{2/3}} \tag{6}$$

  This expression is obtained solely on the assumption that the velocity difference between droplets follows the Kolmogorov self-similarity hypothesis.

  A particularly attractive feature of using this time scale is that it depends explicitly on the liquid volume fraction: $\Lambda = \frac{\bar{\rho}\widetilde{Y_{liq}}}{\rho_{liq}}$

- Obviously, one may use any combination of the above.

Turbulence modelling

Regardless of what particular expression is used for τ_c and r_{eq} it is obvious that accurate calculation of turbulence parameters is needed if one aspires to apply the above atomisation model with an adequate accuracy. Experimental data on turbulence properties in liquid-gas flows are very scarce and because of this the values of measured SMD and droplet number density may be used, up to a point, as basis for the model assessment and validation. Lack of experimental data is even more regrettable if one notes that the two-phase flow is characterised with density ratios which could be as high as 700 (water/air at normal conditions).

Another difficulty is linked to the fact that the equation of state should reflect the very small compressibility of a liquid as compared with a gas:

$$\bar{p} = \frac{\bar{\rho}\left(1 - \widetilde{Y_{liq}}\right) R_g T_g}{1 - \frac{\bar{\rho}\widetilde{Y_{liq}}}{\rho_{liq}}} \tag{7}$$

where the average density is calculated as:

$$\bar{\rho} = \left(\frac{\widetilde{Y_{liq}}}{\rho_{liq}} + \frac{1 - \widetilde{Y_{liq}}}{\rho_g} \right)^{-1} \tag{8}$$

Description of two-phase flow as a single continuum allows one to hope that models developed and tested for gaseous flows with density variations such as premixed flames or light/heavy gas jets, could be used without major alterations. As a departure point the standard $k - \varepsilon$model (Launder and Spalding, 1972) was chosen for this work because of its widespread use especially in engineering applications. It has been found in simulations that the flow reveals a number of recirculation zones, so the renormalisation group $k - \varepsilon$model of Yakhot *et al.* (1992), acclaimedly better for such flows, also has been tried.

However, it is widely recognised, see e.g. Jones (1994), that correlations between density, pressure and velocity fluctuations usually neglected in the $k - \varepsilon$model may be necessary for modelling of a flow with density variations. So the next step in the present research is the addition of such terms following the work of Borghi and Escudie (1984). More

specifically, the following production term in the equation for k has been added:

$$\overline{u_j''}\frac{\partial \bar{p}}{\partial x_j} = \bar{\rho}\widetilde{u_j''Y_{liq}''}\left(\frac{1}{\rho_{liq}} - \frac{1}{\rho_g}\right)\frac{\partial \bar{p}}{\partial x_j} \qquad (9)$$

where $\overline{u_j''}$ is the Reynolds average of velocity fluctuation weighted by density. The average pressure field is calculated with the help of the SIMPLE algorithm.

The large density variations in the flow caused certain difficulties in achieving convergence during numerical solution; very low values of about 0.1 for under-relaxation factors had to be used, this should be compared with 0.5-0.9 used for constant density flows. Moreover, in spite of all efforts, no convergent solution has been obtained so far with Reynolds stress models.

FLOW GEOMETRY

The experiments of Hopfinger and Lasheras (1994) and Lasheras *et al.* (1998), on the atomisation of a water jet by a high-velocity air co-axial jet have been chosen as a test case. An attractive feature of these experiments is that the values of Sauter Mean Diameter (SMD) have been measured for a wide range of independently varied liquid/air velocities. Also the range of conditions studied is a very good approximation to the regimes of air-assisted atomisers widely used, e.g. in gas turbines and rocket engines.

The geometry of atomisers in these two sets of experiments is very similar. In the former, the liquid jet diameter is 3.5 mm, surrounded by an annular coaxial air jet with an outer diameter of 5.6 mm. In the latter, the liquid jet diameter is slightly changed to 3.8 mm. In order to simulate these experiments, a 2D (symmetrical) cylindrical domain with a length of 0.75 m and radius of 0.1 m has been considered with the centre of the coaxial jets located at $x = 0$ and $r = 0$. A non-uniform mesh resolution of 170 by 90 was found to be sufficient. Boundary conditions used were: zero normal derivative for all dependent variables at the outlet $x = 0.75\,m$ and at the upper boundary $r = 0.1\,m$ and uniform velocity and turbulence parameters profiles at the inlet, $l_t = 0.2 \cdot D_{liq}$ in the liquid jet and $l_t = 0.2 \cdot D_g$ in the air jet, $u'/\bar{U} = 5\%$. Symmetry conditions were imposed on axis $r = 0$; non-slip conditions were used for the wall at $x = 0$.

RESULTS AND DISCUSSION

The first simulations were performed with the $k-\varepsilon$model without any special modification accounting for density variations, see Fig. 1. The same flow conditions modelled with the RNG $k-\varepsilon$model lead to a distinctively different pattern, see Fig. 2. The flowfield computed with the $k-\varepsilon$model including pressure gradient effects, Eq. 9, is presented in Fig. 3. On the figures above the grey levels specify the mean liquid mass fraction Y_{liq} with the streamlines superimposed. One can see clearly that a number of large-scale vortices is generated on the air side of the shear layer between the two jets. The effect of the vortex nearest to the injector is to deform the liquid jet, and to produce a visible deviation of the flow pattern from a constant density self-similar jet shape. Moreover, the presence of those vortices means the dependency of turbulence properties on the distance downstream is oscillatory, in striking contrast to gaseous jets, Pietri *et al.* (1996). This is further illustrated in Fig. 5. The flowfields predicted with the three different variants of the $k-\varepsilon$model differ significantly, however, the absence of experimental data makes the choice of the best nearly impossible.

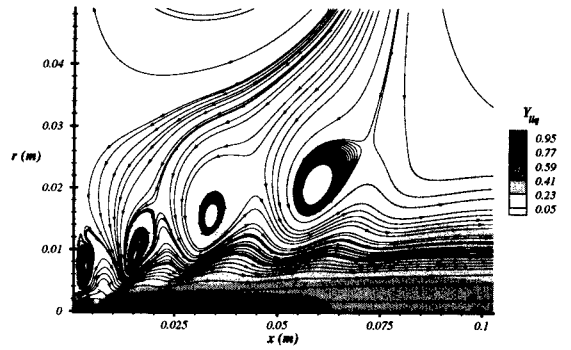

Figure 1: Flowfield and the liquid mass fraction isolines for the case of $u_g = 225\,m/sec$, $u_{liq} = 0.5\,m/sec$. Predictions of the standard $k-\varepsilon$model

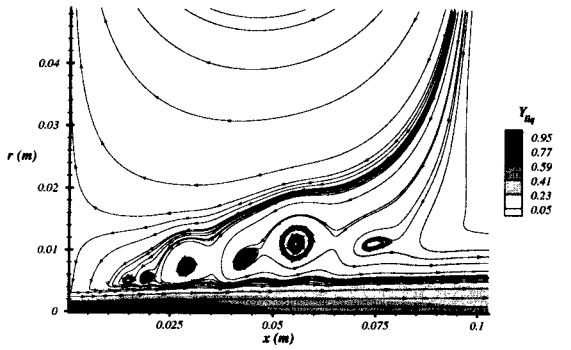

Figure 2: Flowfield and the liquid mass fraction isolines for the case of $u_g = 225\,m/sec$, $u_{liq} = 0.5\,m/sec$. Predictions of the RNG $k-\varepsilon$model

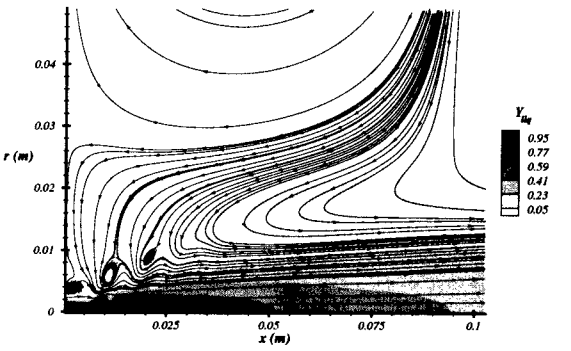

Figure 3: Flowfield and the liquid mass fraction isolines for the case of $u_g = 225\,m/sec$, $u_{liq} = 0.5\,m/sec$. Predictions of $k-\varepsilon$with Eq. 9

In calculations of atomisation using the standard $k-\varepsilon$model, the values of constants recommended in the work of Vallet *et al.* (2001), see Table 1, were adopted and it has been found that though the computed values of SMD agree with measurements in their order of magnitude, the increase in atomising air velocity results in an **increase** of SMD values on the axis, contrary to expectations and measurements, see Fig. 4. Analysis of the computed values of $\tilde{k}$ on the axis show that the standard $k-\varepsilon$model predicts lower values for a higher air jet velocity, see Fig. 5. Such a prediction

Table 1: Values of constants used in simulations.

c_1	c_2	c_3	C_r	Sc_{liq}
0.3	0	0	0.75	0.7

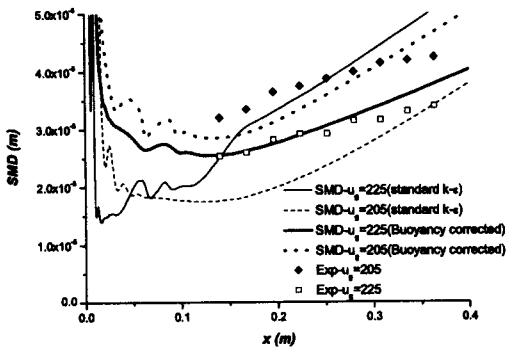

Figure 4: SMD values on axis for the two cases of $u_g = 225$ and $205\,m/sec$, $u_{liq} = 0.5\,m/sec$, standard $k-\varepsilon$and $k-\varepsilon$with Eq. 9

is obviously erroneous because higher air jet velocity means higher shear intensity hence stronger turbulence generation and this presented a further motivation for refinement of the turbulence modelling.

The above-mentioned deficiency of the standard $k-\varepsilon$model seems to be corrected with use of the extra source term, Eq. 9. In Fig. 6 presented are SMD values for

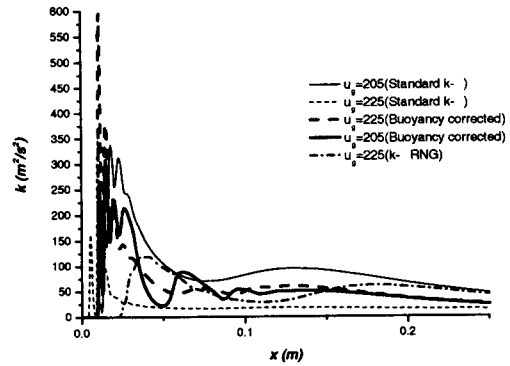

Figure 5: Turbulence kinetic energy on the axis for the two cases of $u_g = 225, 205\,m/sec$ and $u_{liq} = 0.5\,m/sec$ with different turbulence models

two cases with $u_g = 225\,m/s$, $u_{liq} = 0.5\,m/s$ and $u_g = 140\,m/s$, $u_{liq} = 0.55\,m/s$ calculated with the three above-mentioned variants of the $k-\varepsilon$model. Upon comparison with experiments one can see that the RNG $k-\varepsilon$significantly underpredicts SMD values for the first case and greatly overpredicts it for the second case. At the same time, the two other models predictions compare better with experiments. Thus, becasuse the standard $k-\varepsilon$predicted a reverse trend shown in Fig. 4 and also because of a failure to get a converged solution with the more advanced Reynolds stress model, the modified $k-\varepsilon$model was retained for all subsequent calculations.

Surprisingly enough, even a very modest (about ten

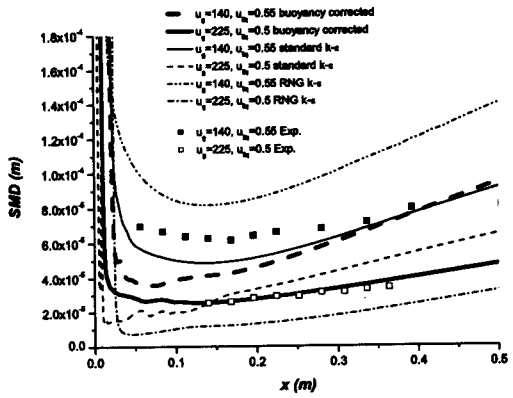

Figure 6: Comparison of calculated SMD values by the three variants of $k-\varepsilon$model with experiments for two cases of $u_g = 225\,m/sec$, $u_{liq} = 0.5\,m/sec$ and $u_g = 140\,m/sec$, $u_{liq} = 0.55\,m/sec$.

percent) decrease in the air velocity results in a quite pronounced change in the flow pattern, see Fig. 7. The first vortex is now generated at about 1 cm downstream from the injector lip as compared to as close a distance as 2 mm in the previous case. It has been observed in gaseous jets that a

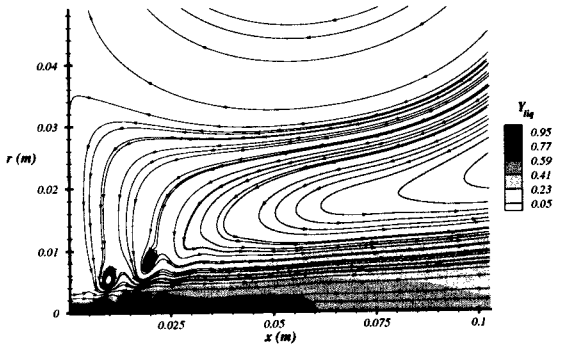

Figure 7: Flowfield and the liquid mass fraction isolines for the case of $u_g = 205\,m/sec$, $u_{liq} = 0.5\,m/sec$. Predictions of the $k-\varepsilon$model with Eq. 9.

recirculation zone may be formed close to the jet exit, Pietri *et al.* (1996) under certain conditions, however, we are unaware of any similar experimental observation for two-phase flows. Obviously, atomisation characteristics would depend on the presence of those recirculation zones. In particular, Figs. 3 and 7 suggest that the presence of a large-scale vortex near the injector affects strongly the liquid core length.

It has been argued, Lasheras *et al.* (1998), that in air-assisted atomisers the atomisation quality is defined by the ratio of gas/liquid flows momentum fluxes

$$M = \frac{\rho_g u_g^2}{\rho_{liq} u_{liq}^2}$$

Such an assumption implicitly presumes that the global flow pattern remains unchanged upon variation of gas or liquid velocity. However, the present results imply that relatively minor change in gas velocity may alter significantly the flow field, and as a consequence, a doubt upon any direct comparison of the two cases would be cast, if a further study confirms the reliability of the results presented above.

The characteristic atomisation rate calculated from Eqs. 4 and 6 is given in Fig. 8. It can be easily seen that in the near-field the Eq. 4 results in faster atomisation, i.e. an increase in the liquid surface area $\tilde{\sigma}$, while further downstream the collision time given by Eq. 6 is approximately two orders of magnitude less that the turbulent integral time scale.

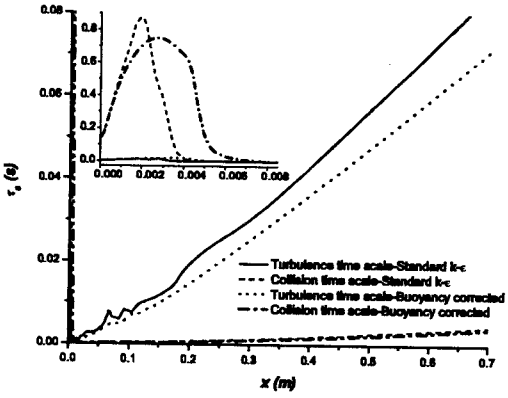

Figure 8: Integral time scale of turbulence and droplet collision time for the case of $u_g = 225\,m/sec$, $u_{liq} = 0.5\,m/sec$.

Figure 9 presents comparison between the equilibrium values of droplet diameter, obtained with Eq. 3, the values of SMD calculated from Eq. 2 and measurements. The τ_c value in Eq. 2 was calculated from Eq. 4; one can see a very rapid initial decrease in r_{eq} for high intensity turbulence near the injector and there the SMD calculated from Eq. 2 "lags behind" the equilibrium values. Further downstream, the turbulence decays and this results in a quite fast increase in r_{eq}; here again, the values of SMD given by Eq. (2) reveal a substantial amount of inertia in following the r_{eq}.

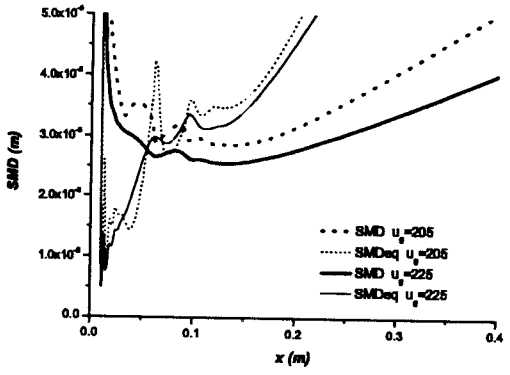

Figure 9: Values of SMD and SMD at equilibrium on axis for the two cases of $u_g = 225\,m/sec$ and$u_g = 205\,m/sec$, $u_{liq} = 0.5\,m/sec$.

The physical mechanism responsible for the r_{eq} increase in the downstream region is droplet coalescence which occurs during their collisions, the rate of these collisions being, obviously, sensitive to the turbulence properties. No appreciable difference has been found between the predictions obtained with Eq. 5 and Eq. 4, however, use of the much faster collision time given by Eq. 6 results in SMD's following closely equilibrium values and, henceforth, increasing faster with the downstream distance than was found in the experiments.

A possible conclusion from a good agreement between measurements and predictions from Eq. 4 would be that droplet motion is collisionless within large-scale structures (streamlines cannot cross) and the collisions happen at the moment of large eddy decay. It is commonly agreed, Launder and Spalding (1972), that the decay rate of large-scale eddies is governed by τ_t.

As another test of the performance of the $k-\epsilon$with the extra generation term, Eq.9, calculations have been performed for 5 cases with a constant gas velocity of $u_g = 140\,m/s$ and liquid velocities varying from 0.13 m/s to 0.55 m/s. Comparison with appropriate experimental values of SMD, Lasheras *et al.* (1998), can be found in Fig. 10. As one can see, in all cases calculations follow the same trend as experiments, i.e. SMD increases with increase of liquid jet velocity. The predicted values are also reasonably close to measured ones.

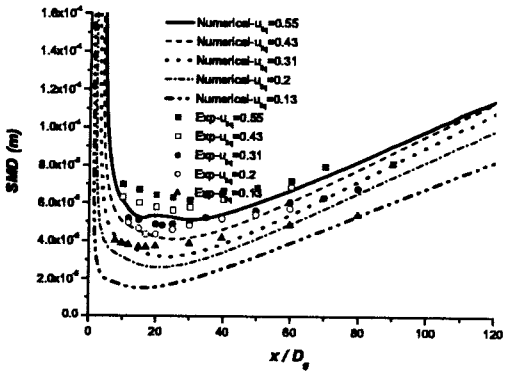

Figure 10: SMD values on axis for five cases with $u_g = 140\,m/sec$ and $u_{liq} = 0.13, 0.2, 0.31, 0.43, 0.55\,m/sec$ compared with experiments.

Still, though the results are encouraging, they are not perfect, because the spread rate is under-predicted by all three models employed, see Fig. 11. Once more, the RNG $k-\epsilon$proves to be the worst of all three models.

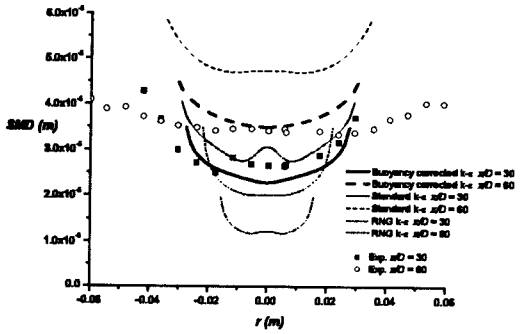

Figure 11: Radial profiles of droplet SMD for the case of $u_g = 225\,m/sec$, $u_{liq} = 0.5\,m/sec$.

The last observation which can be deduced from Figs. 3 and 7 is that it is quite possible that the flow in question has a non-steady behaviour, and there exists a periodic vortex shedding in the layer between the jets. Answers to this question require non-steady calculations which will be the subject of future work.

CONCLUSIONS

Three different modifications of the $k-\varepsilon$model have assessed in order to find the most appropriate for predicting the atomisation of liquid jets. It has been found that the large density ratio in the flow makes the usually neglected correlation between pressure gradients and velocity an important source of turbulence production. It has also been found that a number of strong vortices are formed on the outer edge of the atomising air flow, and this obviously has an impact on calculated values of droplet SMD. It has proved possible to achieve a reasonable agreement with experiments in terms of droplet SMD on the symmetry axis of the flow. However, the spray jet spread rate is predicted poorly and this affects the comparison with radial profiles.

ACKNOWLEDGMENTS

The financial support of EPSRC is gratefully acknowledged.

REFERENCES

Borghi R., Escudie D., 1984, "Assessment of a theoretical model of turbulent combustion by comparison with a simple experiment", *Combustion and Flame*, Vol.56, pp. 149-164.

Borghi R., 1988, "Turbulent combustion modelling", *Progr. Energy Combust. Sci.*, vol. 14, p. 245.

Hopfinger E.J., Lasheras J.C., 1994, "Breakup of a water jet in high velocity co-flowing air", ICLASS-94, Rouen, France, pp. 110-117.

Jones W.P., 1994, "Turbulence modelling and numerical solution methods for variable density and combusting flows", in *Turbulent Reacting Flows*, Libby P.A., Williams F.A., eds. , Academic Press, London, pp. 309-368.

Kolmogorov A.N., 1949, "On the disintegration of drops by turbulent flows", *Doklady Akademii Nauk SSSR*, Vol. 66, pp. 825-828.

Lasheras J.C., Villermaux E. and Hopfinger E.J., 1998, "Break-up and atomisation of a round water jet by a high speed annular air jet", *J. Fluid Mech.*, vol. 357, pp.351-379.

Launder B.E., Spalding D.B., 1972, "Lectures in mathematical models of turbulence", Academic Press, London.

Lefebvre A.H., 1989, "Atomization and Sprays", Hemisphere publ., N.Y.

Pietri L., Amielh M., Anselmet F. and Fulachier L., 1996, "Velocity turbulence properties in the near-field region of axisymmetric variable density jets", *Phys. Fluids,* vol. 8, pp. 1614-1630.

Vallet A., Burluka A.A. & Borghi R., 2001, "Development of an eulerian model for the "atomisation" of a liquid jet", *Atomization and Sprays*, vol. 11, pp. 619-642.

Yakhot V., Orszag S.A., Thangam S., Gatski T.B., Speziale C.G., 1992, "Development of turbulence models for shear flows by a double expansion technique", Phys. Fluids, Vol. 4, pp. 1510-1520.